Acta Crystallographica Section B
Structural Science
ISSN 0108-7681

Temperature dependence of the silver distribution in the crystal structure of natural pearceite, $(Ag,Cu)_{16}(As,Sb)_2S_{11}$

Luca Bindi,[a]* Michel Evain[b] and Silvio Menchetti[a]

[a]Dipartimento di Scienze della Terra, Università di Firenze, Via La Pira 4, 50121 Firenze, Italy, and [b]Laboratoire de Chimie des Solides, IMN, UMR C6502 CNRS, Université de Nantes, 2 rue de la Houssinière, BP32229, 44322 Nantes CEDEX 3, France

Correspondence e-mail: lbindi@geo.unifi.it

Received 27 September 2005
Accepted 10 January 2006

The crystal structure of the mineral pearceite, $(Ag,Cu)_{16}(As,Sb)_2S_{11}$, has been solved and refined at 300, 120 and 15 K. At room temperature pearceite crystallizes with trigonal symmetry, space group $P\bar{3}m1$; the refinement of the structure leads to a residual factor of R = 0.0464 for 1109 independent observed reflections and 92 variables. The crystal structure consists of sheets stacked along the c axis. The As atoms form isolated $(As,Sb)S_3$ pyramids, which typically occur in sulfosalts, copper cations link two S atoms in a linear coordination, and the silver cations are found in a fully occupied position and in various sites corresponding to the most pronounced probability density function locations (modes) of diffusion-like paths. These positions correspond to low-coordination (2, 3 and 4) sites, in agreement with the preference of silver for such environments. d^{10} silver-ion distribution has been determined by means of a combination of a Gram–Charlier description of the atomic displacement factors and a split-atom model. To analyse the crystal chemical behaviour of the silver cations as a function of temperature, a structural study was carried out at 120 K (R = 0.0450). The refinement indicates that the mineral exhibits the same structural arrangement as the room-temperature structure (space group $P\bar{3}m1$) and shows that the silver cations are still highly disordered. In order to investigate a possible ordering scheme for the silver cations, a data collection at ultra-low temperature (15 K) was performed. The structural skeleton was found to be similar to that of the room-temperature and 120 K atomic structures, but the best solution was achieved with a fully split-atom model of five silver positions, giving an R value of 0.0449 for 651 observed reflections and 78 parameters. Although the silver cation densities condense into better defined modes, the joint probability density function still exhibits a strong overlapping of neighbouring sites.

1. Introduction

Silver chalcogenides have received much attention in recent years because of their important technological applications. These compounds, indeed, are known to be fast ionic conductors or semiconductors and as such find practical applications in silver photography as sensitizers and in optics and microelectronics as rewritable storage media. In order to understand these properties, an exact knowledge of the crystal structure of the compound is indispensable.

According to Frondel (1963) and Hall (1967), the minerals belonging to the pearceite–polybasite series can be divided into two sub-series; the first, formed by pearceite, $(Ag,Cu)_{16}$-

Table 1
Electron microprobe data (means and ranges in wt% of elements) and atomic ratios with their standard deviations (σ) for the selected pearceite crystal.

	wt%	Range	Atomic ratios	σ
Ag	62.34	58.85–63.25	12.15	0.13
Cu	11.60	11.11–12.08	3.84	0.08
As	4.19	3.99–4.33	1.18	0.03
Sb	4.82	4.55–5.01	0.83	0.04
S	16.77	16.33–17.11	11.00	0.09
Total	99.72	99.61–100.59		

$(As,Sb)_2S_{11}$, and antimonpearceite, $(Ag,Cu)_{16}(Sb,As)_2S_{11}$, is characterized by a 'small' unit cell (labelled 111) and high Cu content, and the second, formed by polybasite, $(Ag,Cu)_{16}(Sb,As)_2S_{11}$, and arsenpolybasite, $(Ag,Cu)_{16}(As,Sb)_2S_{11}$, has doubled cell parameters (labelled 222) and low Cu content. The members of both series are reported as monoclinic (Peacock & Berry, 1947; Frondel, 1963; Harris *et al.*, 1965; Hall, 1967; Edenharter *et al.*, 1971), although dimensionally pseudo-hexagonal, with the space group *C*2/*m*. Moreover, Harris *et al.* (1965) and Edenharter *et al.* (1971) pointed out the existence of an intermediate type of unit cell labelled 221 for a sample from Las Chispas Mine, Sonora, Mexico. However, these authors observed that the intermediate cell 221, present in some areas of the sample analysed, was closely associated with the small cell 111 present in other seemingly identical areas of the same sample. By means of an experimental study, Hall (1967) hypothesized that the variation of Cu content in different samples might play a key role in favouring order–disorder (OD) phenomena.

Despite the fact that the minerals belonging to the pearceite–polybasite series are relatively common in nature, no crystal structure characterization has been published so far. One reason for this lack of structural information is probably the difficulty in efficiently describing the Ag or Cu electron density, which is influenced by the strong ionic conductivity of these minerals. It was shown that, for such a description, a non-harmonic model based on a development of the atomic displacement factor seems the most appropriate approach (Kuhs & Heger, 1979; Boucher *et al.*, 1992, 1993; Evain *et al.*, 1998).

In this study we report the crystal structure of a pearceite crystal having the chemical composition $(Ag_{12.15}Cu_{3.84})_{\Sigma=15.99}(As_{1.18}Sb_{0.83})_{\Sigma=2.01}S_{11.00}$ and its low-temperature behaviour in the range 300–15 K.

2. Occurrence and chemical composition

The sample containing the pearceite crystal used in the present study (Museo di Storia Naturale, Sezione di Mineralogia e Litologia, Università di Firenze, Italy, catalogue number 45895/G) is from the Clara Mine, Black Forest, Germany, a well known source of silver-bearing minerals. Pearceite occurs as black anhedral-to-subhedral grains of up to 200 µm in length and shows a grey–black-to-black streak. The other mineral spatially associated with pearceite is stibnite.

A preliminary chemical analysis using energy-dispersive spectrometry, performed on the same crystal fragment used for the structural study at 15 K, did not indicate the presence of elements ($Z > 9$) other than Ag, Cu, As, Sb and S. The chemical composition was then determined using wavelength-dispersive analysis (WDS) by means of an ARL-SEMQ electron microprobe. Major and minor elements were determined at 20 kV accelerating voltage and 40 nA beam current, with 30 s counting time. For the WDS analyses the following lines were used: Ag $L\alpha$, Cu $K\alpha$, Sb $L\beta$, As $L\alpha$ and S $K\alpha$. The estimated analytical precision is ±0.40 for Ag, ±0.30 for Cu and Sb, and ±0.20 for As and S. The standards employed were Ag pure element (Ag), Cu pure element (Cu), Sb pure element (Sb), As pure element (As) and S pure element (S). The pearceite fragment was found to be homogeneous within analytical error. The average chemical composition (seven analyses on different spots), together with ranges of wt% of elements, is reported in Table 1. On the basis of 29 atoms, the formula can be written as $(Ag_{12.15}Cu_{3.84})_{\Sigma=15.99}(As_{1.18}Sb_{0.83})_{\Sigma=2.01}S_{11.00}$.

3. Experimental

Several crystals of pearceite were selected from the 45895/G sample and examined by means of an Enraf–Nonius CAD-4 single-crystal diffractometer using graphite-monochromated Mo $K\alpha$ radiation, and with an Oxford Diffraction Xcalibur 2 diffractometer, fitted with a Sapphire 2 CCD detector. The pearceite crystals were very brittle and showed a soft platy nature. In fact, most of them produced diffraction effects typical of multiple crystallites. A crystal of relatively high diffraction quality was selected for the structural study.

3.1. Data collection at 300 and 120 K

Room-temperature (RT, *ca* 300 K) X-ray diffraction data collection was carried out on both the Oxford Diffraction Xcalibur 2 diffractometer and a Bruker–Nonius KappaCCD diffractometer. Only results obtained with the KappaCCD diffractometer are reported here, since this data set covers much higher $\sin(\theta)/\lambda$ values. To observe an expected localization of the Ag cations (see below), a second measurement was performed at *ca* 120 K on the same crystal with the Bruker–Nonius KappaCCD diffractometer, the low temperature being achieved by means of an Oxford Cryostream cooler. Diffraction patterns at 300 and 120 K were consistent with trigonal symmetry ($a \simeq 7.4$ Å and $c \simeq 11.8$ Å). Given the disorder of some atoms in the structure framework (see below), a high $\sin(\theta)/\lambda$ cut off (0.9 Å^{-1}) and a high redundancy (> 15) were chosen.

3.2. Data collection at 15 K

Owing to the fact that the expected silver localization was not obvious at 120 K (see below) and at 90 K (data set not reported in this paper), data collection at a much lower

temperature (15 K) was initiated. Since the first crystal used for the RT and 120 K measurements was lost during polishing (for analysis purpose), a second suitable crystal from the same rock sample was chosen for the 15 K measurement. The data collection was carried out with an Oxford Diffraction Xcalibur 2 diffractometer, fitted with a Sapphire 2 CCD detector, equipped with a Helijet cooling device. No symmetry change was detected, the diffraction pattern still being compatible with trigonal symmetry and cell parameters $a \simeq 7.4$ Å and $c \simeq 11.8$ Å.

4. Data processing and structure determination

Intensity integration and a standard Lorentz polarization correction were performed with the Bruker–Nonius *EvalCCD* (Duisenberg*et al.*, 2003) program package (RT and 120 K) and with the *CrysAlis* (Oxford Diffraction, 2002) software package (15 K). Except for the direct methods tests carried out with the *SHELX* software (Sheldrick, 1997), all calculations were conducted using the *JANA2000* program suite (Petrícek & Dusek, 2000). The sets of reflections were corrected for absorption *via* a Gaussian analytical method, after a shape and dimension optimization with *X-SHAPE* (Stoe & Cie, 1996) based on the *HABITUS* program (Herrendorf, 1993). The structure drawings were realized with the *DIAMOND* program (Brandenburg, 2001) and the *IRIS EXPLORER* visualization program (Numerical Algorithms Group, Downers Grove, IL, USA) running on a Compaq DS20 computer.

4.1. Structure determination and refinement at 300 K

No particular systematic extinctions were observed at RT, allowing $P\bar{3}m1$ as a possible space group. The merging of data according to the $\bar{3}m1$ point group led to the internal R value $R_{\rm int} = 0.048$ for all reflections. A first partial solution was found with the *SHELXS97* direct methods (Sheldrick, 1997). It was soon realized that some atoms were highly disordered, particularly Ag atoms in a diffusion-like layer at *ca* $z = 0.12$. Accordingly, split atoms were successively added at the positions found in the Fourier difference syntheses. However, no matter what the number of additional atom sites it was not possible to obtain a residual value lower than *ca* $R = 0.07$, with residues ranging from −4.4 to 6.6 e Å^{-3} around Ag atoms and correlations as high as 0.99. Since the symmetry of the minerals was previously reported as monoclinic (see above), a different solution was then sought in that crystal system, with concomitant twinning laws. Many trials involving various structure/space group combinations were tested, but they did not improve the $F_{\rm obs}$ *versus* $F_{\rm calc}$ agreement. Returning to the trigonal system, space group $P\bar{3}m1$, a non-harmonic approach with a Gram–Charlier description of the Debye–Waller factor (Johnson & Levy, 1974; Kuhs, 1984) was then attempted, with the aim of reducing both the number of refined positions and the correlations, and of converging to a reasonable structure model. Such an approach has already been used with success on many occasions, for instance in the argyrodite family (Boucher *et al.*, 1993). A major improvement was achieved, on the one hand, by introducing up to fourth-order tensors for the mixed Ag1/Cu1 position and its coordinating S4 position. A stable model with correlation coefficients lower than 0.9 for the silver 'diffusion-like' joint probability density function (JPDF) within the S1–S2–S3 tetrahedron-based framework was found, on the other hand, by using only two silver positions: Ag2 with regular anisotropic atomic displacement parameters and Ag3 with higher-order tensors up to fourth order (see Fig. 1). The absence of significant negative regions in the probability density function (PDF; holes less than 4% of the peaks, in absolute value), the small R value and the low residues (from −1.0 to 1.4 e Å^{-3}) support the validity of the model. Adding an equation on the global Ag occupation to fulfil the overall charge balance, imposing full-site occupancy restrictions for As/Sb and Ag1/Cu1, and introducing a secondary extinction coefficient (Becker & Coppens, 1974), allowed the residual R value to smoothly converge to 0.0464 for 1109 reflections [$I > 2\sigma(I)$] and 92 parameters. It is worth noting that a refinement without restrictions on the overall charge balance leads to exactly the same R value, but with a slight positive charge excess (0.07 per formula unit).

4.2. Structure determination and refinement at 120 K

Starting from the RT structure model, the refinement of the 120 K structure smoothly converged to $R = 0.056$. An improvement of the agreement was obtained by introducing a split-atom model for S4 instead of the non-harmonic approach, S4 being moved away from its highly symmetric position, and by adding a new silver position (Ag4, anisotropic) in the 'diffusion-like' silver layer (see Fig. 1). Although similar to the RT values when refined, the As/Sb and Ag1/Cu1 ratios were fixed, for coherence, to those obtained in the RT refinement. With a secondary extinction coefficient, the final residual value reached $R = 0.045$ for 1167 observed reflections and 96 parameters.

4.3. Structure determination and refinement at 15 K

With the 120 K structure as a starting point, good agreement was quickly obtained for the 15 K data set. The crystal being different from that used for the RT and 120 K structure determination (see above), the As/Sb and Ag1/Cu1 ratios were once again refined but with full site-occupancy restrictions. With a skeleton similar to that of the RT and 120 K atomic structures, different solutions were tested for the modelling of the 'diffusion-like' silver layer. Although a non-harmonic approach was still possible, the best solution (lower correlation, fewer parameters and lower R value) was found with a fully split-atom model of five positions (see Fig. 1), three of them (Ag2, Ag3 and Ag5) with isotropic atomic displacement parameters (ADPs) and the remaining positions (Ag4 and Ag6) with anisotropic ADPs. Notice that with fewer data [$\sin(\theta)/\lambda$ being limited to 0.77 for technical reasons], the ADPs are slightly less accurate. A final R value of 0.0449 was obtained for 651 reflections and 78 parameters. Crystal characteristics, data collection and reduction parameters, and

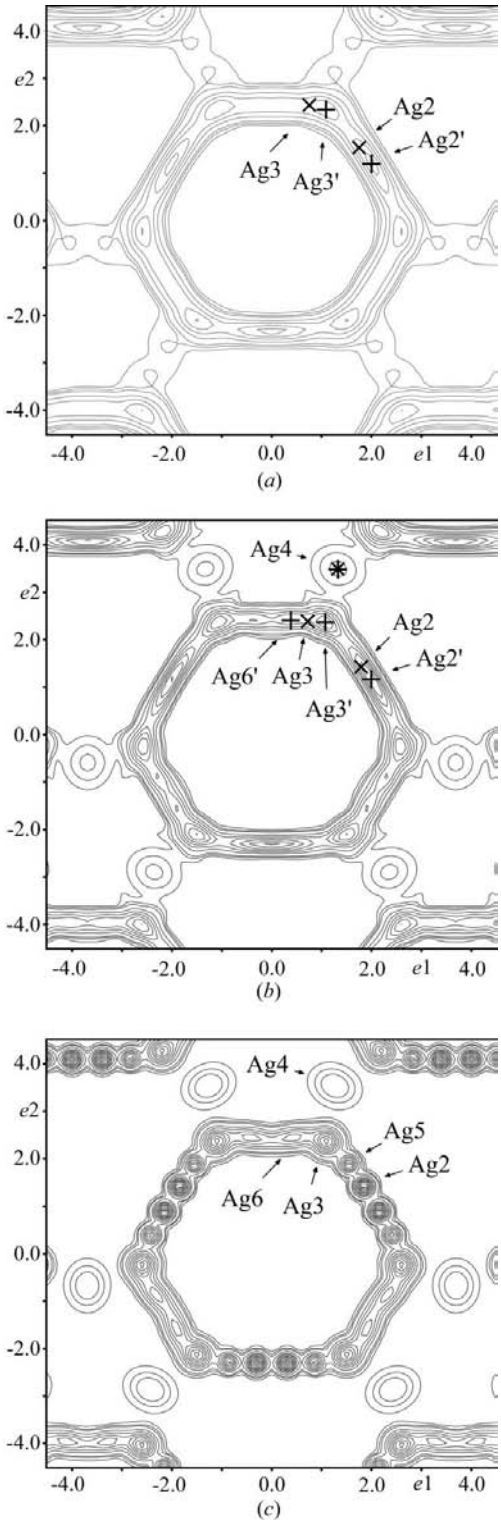

Figure 1
Non-harmonic joint probability density function maps showing the silver localization as a function of temperature: (*a*) 300, (*b*) 120 and (*c*) 15 K. Maps, in Å, are centred at (0, 0, 0.12) and summed over Δz = 2 Å. Contour lines are for 0.02 and 0.04 Å^{-3}, and then from 0.06 Å^{-3} to a maximum of 0.32, 0.42 and 0.65 Å^{-3} for 300, 120 and 15 K, respectively, in intervals of 0.06 Å^{-3}. Refined positions are indicated by × and calculated mode positions by +. Negative values are not indicated with contour levels, since they are lower, in absolute value, than 4 and 6.5% of the maximum at 300 and 120 K, respectively.

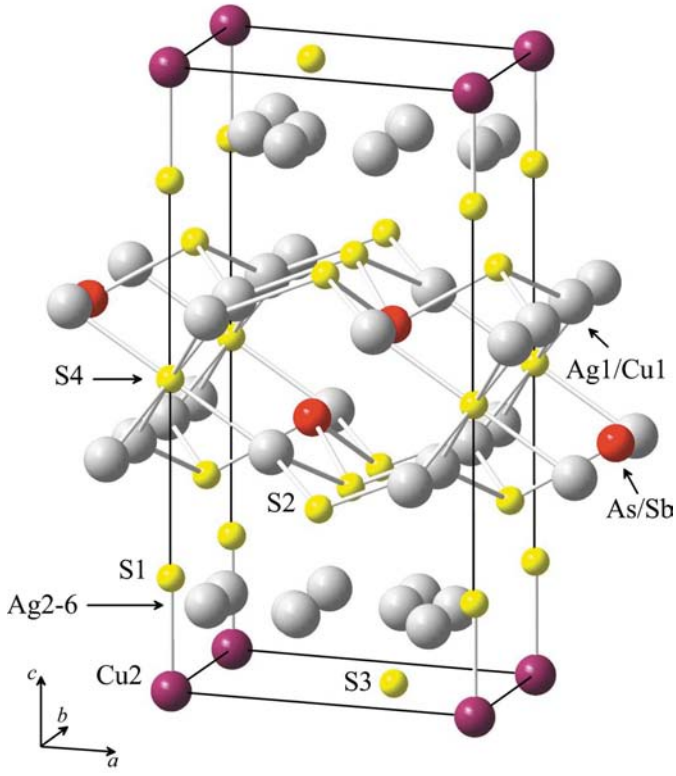

Figure 2
Structure of $(Ag,Cu)_{16}(As,Sb)_2S_{11}$, showing the stacking of the $[(Ag,Cu)_6(As,Sb)_2S_7]$ and $[Ag_9CuS_4]$ layers (see text). The positions in the Ag2–6 layer are those from the RT structure (*i.e.* Ag2 and Ag3), and the S4 position is indicated by only one atom.

refinement results are gathered in Table 2. Atomic parameters are reported in Table 3 and in the supplementary material.[1]

5. Description and discussion of the structure

The crystal structure of pearceite (Fig. 2) consists of sheets stacked along the *c* axis, where (As,Sb) atoms form $(As,Sb)S_3$ pyramids, which typically occur in sulfosalts, and a Cu atom links two S atoms in a linear coordination. The silver cations are found in a fully occupied position, labelled Ag1/Cu1, and in various sites corresponding to the most pronounced PDF locations (modes) of diffusion-like paths, labelled Ag2–6. These positions correspond to low-coordination sites (2, 3 and 4), in agreement with the preference of silver for such environments. Basically, although not a layered compound, the structure of $(Ag,Cu)_{16}(As,Sb)_2S_{11}$ can be easily described as a regular alternation of two kinds of layers along [001]: a first layer (labelled *A*), ~6.15 Å thick, with the general composition $[(Ag,Cu)_6(As,Sb)_2S_7]^{2-}$, and a second layer (labelled *B*), 5.75 Å thick, with the general composition $[Ag_9CuS_4]^{2+}$.

[1] Supplementary data for this paper are available from the IUCr electronic archives (Reference: LC5042). Services for accessing these data are described at the back of the journal.

Table 2
Experimental details.

	300 K	120 K	15 K
Crystal data			
Chemical formula	$Ag_{13.03}As_{1.18}Cu_{2.97}S_{11}Sb_{0.82}$	$Ag_{13.03}As_{1.18}Cu_{2.97}S_{11}Sb_{0.82}$	$Ag_{12.21}As_{1.19}Cu_{3.79}S_{11}Sb_{0.81}$
M_r	2135.4	2135.4	2098.2
Cell setting, space group	Trigonal, $P\bar{3}m1$	Trigonal, $P\bar{3}m1$	Trigonal, $P\bar{3}m1$
Temperature (K)	300	120	15
a, b, c (Å)	7.3876 (4), 7.3876 (4), 11.8882 (7)	7.3721 (6), 7.3721 (6), 11.8104 (12)	7.3890 (10), 7.3890 (10), 11.816 (2)
α (°)	90	90	90
V (Å^3)	561.89 (5)	555.88 (9)	558.69 (14)
Z	1	1	1
D_x (Mg m^{-3})	6.309	6.377	6.234
Radiation type	Mo $K\alpha$	Mo $K\alpha$	Mo $K\alpha$
μ (mm^{-1})	17.51	17.70	17.68
Crystal form, colour	Prism, black	Prism, black	Prism, black
Crystal size (mm)	0.04 × 0.15 × 0.15	0.04 × 0.15 × 0.15	0.15 × 0.16 × 0.18
Data collection			
Diffractometer	Bruker–Nonius KappaCCD	Bruker–Nonius KappaCCD	Oxford Diffraction Xcalibur 2
Data collection method	ω scans	φ and ω scans	ω scans
Absorption correction	Gaussian	Gaussian	Gaussian
T_{min}	0.197	0.165	0.069
T_{max}	0.727	0.659	0.158
No. of measured, independent and observed reflections	20 965, 1352, 1109	17 722, 1341, 1167	2442, 818, 650
Criterion for observed reflections	$I > 2\sigma(I)$	$I > 2\sigma(I)$	$I > 2\sigma(I)$
R_{int}	0.048	0.048	0.051
θ_{max} (°)	40.0	40.0	33.1
Range of h, k, l	$-13 \Rightarrow h \Rightarrow 13$ $-12 \Rightarrow k \Rightarrow 12$ $-21 \Rightarrow l \Rightarrow 21$	$-12 \Rightarrow h \Rightarrow 13$ $-13 \Rightarrow k \Rightarrow 13$ $-20 \Rightarrow l \Rightarrow 21$	$-11 \Rightarrow h \Rightarrow 10$ $-9 \Rightarrow k \Rightarrow 10$ $-4 \Rightarrow l \Rightarrow 18$
Refinement			
Refinement on	F^2	F^2	F^2
$R[F^2 > 2\sigma(F^2)]$, $wR(F^2)$, S	0.046, 0.127, 1.89	0.045, 0.133, 2.19	0.044, 0.126, 1.84
No. of reflections	1352	1341	818
No. of parameters	92	96	77
Weighting scheme	Based on measured s.u.s, $w = 1/[\sigma^2(I) + 0.001936I^2]$	Based on measured s.u.s, $w = 1/[\sigma^2(I) + 0.001936I^2]$	Based on measured s.u.s, $w = 1/[\sigma^2(I) + 0.001936I^2]$
$(\Delta/\sigma)_{max}$	<0.0001	0.001	0.001
$\Delta\rho_{max}$, $\Delta\rho_{min}$ (e Å^{-3})	1.41, −1.00	1.57, −1.86	1.54, −1.48
Extinction method	B–C type 1 Gaussian isotropic (Becker & Coppens, 1974)	B–C type 1 Lorentzian isotropic (Becker & Coppens, 1974)	B–C type 1 Lorentzian isotropic (Becker & Coppens, 1974)
Extinction coefficient	0.29 (6)	0.39 (8)	0.01 (2)

5.1. The *A* layer

The *A* layer of the crystal structure of pearceite contains the only fully occupied position for the Ag atoms. This fully occupied position, labelled Ag1/Cu1, is triangularly coordinated by S atoms (two S2 and one S4), showing bond distances ranging from 2.359 (2) to 2.446 (2) Å. The average bond distance of 2.417 Å is in agreement with a partial substitution of copper for silver at this site. It is worth noting that the Ag1/Cu1—S4 distances correspond to the most probable distances given by the four S4 split positions (120 and 15 K). The combination of the Ag and Cu PDFs, in addition to a probable static and/or dynamic disorder as observed, for instance, for Cu in the similar environment of the synthetic tetrahedrite $Cu_{12}Sb_4S_{13}$ (Pfitzner *et al.*, 1997), makes the overall site PDF very complicated in shape. This explains the fact that the Ag1/Cu1 distribution could not be properly explained by a split-atom model and required a non-harmonic approach. It also explains the observed splitting of the S4 position, which was not necessary in the structure refinement of $Cu_{12}Sb_4S_{13}$, where one finds an identical coordination for sulfur.

The (As,Sb) atoms are in a threefold coordination occupying the top of a trigonal pyramid, with three S atoms forming the base. $(As,Sb)S_3$ polyhedra are isolated from each other but linked to $(Ag1/Cu1)S_3$ units to constitute a layer and not a three-dimensional structure as in $Cu_{12}Sb_4S_{13}$ (Pfitzner *et al.*, 1997). The (As,Sb)—S average bond distance of 2.316 (1) Å is consistent with the value obtained by considering the ⟨As—S⟩ and the ⟨Sb—S⟩ bonds of the pure proustite, $Ag_3[AsS_3]$, and pyrargyrite, $Ag_3[SbS_3]$ (2.293 and 2.452 Å, respectively; Engel & Nowacki, 1966). Indeed, taking into account the molar fractions of As and Sb in pearceite [*i.e.* As =

Table 3
Non-harmonic displacement parameters and s.u. values for the selected pearceite crystal.

Third-order tensor elements C^{ijk} are multiplied by 10^3. Fourth-order tensor elements D^{ijkl} are multiplied by 10^4.

	300 K			120 K		15 K
	Ag1/Cu1	Ag3	S4	Ag1/Cu1	Ag3	Ag1/Cu1
D^{1111}	−0.0076 (16)	−0.19 (2)	−0.54 (3)	−0.0146 (8)	−0.150 (6)	−0.018 (2)
D^{1112}	−0.0038 (8)	0.148 (18)	−0.269 (13)	−0.0073 (4)	0.026 (2)	−0.0092 (12)
D^{1113}	0.0060 (5)	0.062 (4)	−0.001 (4)	0.0074 (3)	0.0307 (15)	0.0067 (7)
D^{1122}	−0.0028 (5)	0.203 (15)	−0.269 (13)	−0.0055 (3)	0.0042 (14)	−0.0074 (9)
D^{1123}	0.0030 (2)	0.006 (2)	−0.0003 (19)	0.00369 (14)	−0.0028 (5)	0.0034 (4)
D^{1133}	−0.00212 (19)	−0.0105 (9)	−0.0002 (12)	−0.00298 (13)	−0.0049 (4)	−0.0032 (3)
D^{1222}	−0.0023 (9)	0.226 (15)	−0.269 (13)	−0.0046 (4)	−0.0005 (11)	−0.0065 (15)
D^{1223}	0.00182 (16)	0.000 (2)	0.0003 (19)	0.00241 (9)	−0.0006 (3)	0.0026 (3)
D^{1233}	−0.00106 (9)	−0.0011 (4)	−0.0001 (6)	−0.00149 (7)	0.00049 (14)	−0.00162 (15)
D^{1333}	0.00111 (12)	0.0011 (2)	0	0.00115 (7)	0.00061 (11)	0.00106 (16)
D^{2222}	−0.0026 (7)	0.213 (16)	−0.54 (3)	−0.0046 (4)	−0.0018 (12)	−0.0057 (16)
D^{2223}	0.0012 (3)	−0.004 (2)	0.001 (4)	0.00177 (16)	−0.0004 (3)	0.0023 (5)
D^{2233}	−0.00082 (10)	0.0002 (4)	−0.0002 (12)	−0.00104 (6)	0.00003 (13)	−0.00131 (18)
D^{2333}	0.00055 (6)	0.00005 (17)	0	0.00058 (4)	−0.00011 (8)	0.00053 (8)
D^{3333}	−0.00012 (11)	0.00010 (13)	−0.0002 (3)	−0.00022 (6)	−0.00015 (7)	−0.00036 (16)

0.59 and Sb = 0.41 a.f.u. (atoms per formula unit)] and the mean bond distances for the pure components, we obtain a value of 2.358 Å.

5.2. The *B* layer

It should be noted that rather large equivalent displacement parameters are observed for both the sulfur positions, S1 [U_{eq} = 0.0267 (4) Å^2] and S3 [U_{eq} = 0.0428 (6) Å^2], forming the *B* layer. These atomic displacement parameters are related to the silver distribution along what looks like a diffusion path. Owing to this distribution, only overlapping PDFs can be obtained from the single-crystal X-ray structure determination, and the atomic positions refined to model the electronic density, *i.e.* the mean positions, have no geometrical meanings. For this reason and in order to analyse the various crystal chemical environments for such cations, one should use the maxima, corresponding to the mode positions (calculated with *JANA2000*), which can be located in the JPDF (see Fig. 1 and Table 4 for the mode positions). Fig. 3 presents an isosurface of the JPDF of the Ag atoms (Ag2–Ag6) around the Cu2 atom. It clearly shows a diffusion-like path, which constitutes a double layer around the Cu2 atom. Along the silver diffusion-like path, two non-symmetry-related density maxima, Ag2 (mode Ag2*) and Ag3 (mode Ag3*), are found at RT and 120 K. A set of meaningful distances, calculated from the mode positions, is gathered in Table 4. Since the silver positions at room temperature and at 120 K refer to calculated mode positions (thus the absence of s.u. values in Table 4), we will refer to the refined positions Ag2, Ag3, Ag4, Ag5 and Ag6 at 15 K in the description of the *B* layer of the crystal structure of pearceite.

The Ag2 position exhibits a quasi-linear coordination showing two short bond distances at 2.325 (3) and 2.429 (3) Å with S3 and S1, respectively. However, the coordination sphere of Ag2 is completed by two additional bonds with S2 [2.880 (4) and 3.263 (5) Å] and by a short contact with Cu2 at 2.750 (2) Å (Fig. 4*a*). The Ag3 position shows a regular tetrahedral environment, with distances ranging from 2.622 (4) to 2.802 (7) Å (Fig. 4*b*). The average bond distance of 2.717 Å compares well with that found for the Ag3 position in the crystal structure of stephanite, $Ag_5[S|SbS_3]$ (2.68 Å; Ribár & Nowacki, 1970), and that found for the Ag3 polyhedron in the crystal structure of the synthetic $Ag_7S_2[AsS_4]$ (2.642 Å; Pertlik, 1994). Ag4 exhibits a quasi-linear coordi-

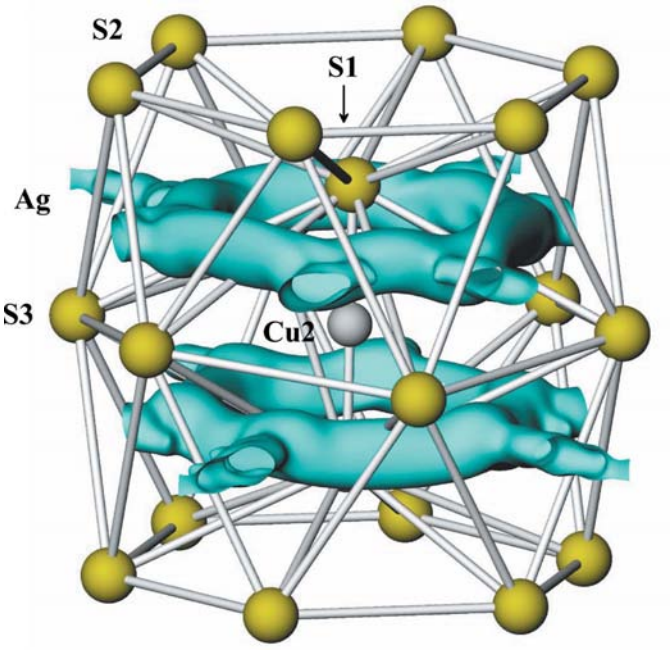

Figure 3
Non-harmonic joint probability density isosurface for silver at RT in the $[Ag_9CuS_4]$ layer extended with S2 atoms, exhibiting the silver diffusion in the *ab* plane. Level of the map: 0.05 Å^{-3}. S and Cu atoms are shown at arbitrary sizes.

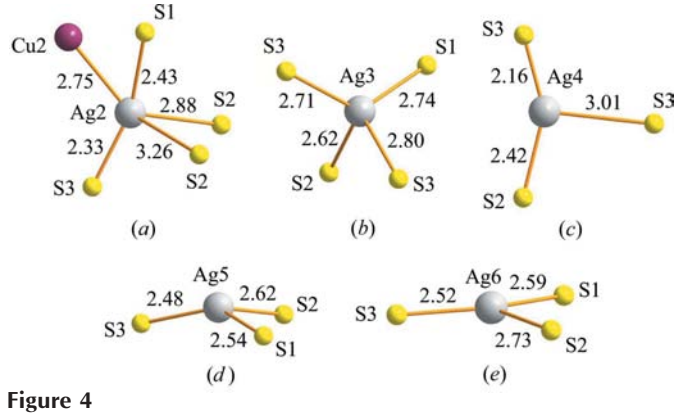

Figure 4
Crystal chemical environments for the Ag2–6 (*a*)–(*e*) cations in the *B* layer of the crystal structure of pearceite (distances in Å).

Table 4
Main interatomic distances (Å) and s.u. values for the selected pearceite crystal.

Positions labelled with an asterisk (*) refer to calculated mode positions (thus the absence of s.u. values), except at 15 K, where Ag2*, Ag3*, Ag5* and Ag6* refer to the corresponding Ag2, Ag3, Ag5 and Ag6 refined positions.

	RT	120 K	15 K
As/Sb—S1	2.3157 (10) × 3	2.3161 (11) × 3	2.341 (2)
Ag1/Cu1—S4†	2.3592 (15)	2.4272 (18)	2.428 (3)
As/Sb—S2	2.4459 (14)	2.4469 (13)	2.453 (2)
As/Sb—S2	2.446 (2)	2.4469 (17)	2.453 (3)
As/Sb—S1	3.0927 (18)	3.0638 (17)	3.064 (3)
Cu2—S1	2.1594 (15) × 2	2.1610 (16) × 2	2.161 (3) × 2
Cu2—Ag2*	2.837	2.731	2.750 (2)
Ag2*—S3	2.239	2.299	2.325 (3)
Ag2*—S1	2.516	2.411	2.429 (3)
Ag2*—S2	3.054 × 2	3.065 × 2	2.880 (4)
Ag2*—S2			3.263 (5)
Ag3*—S2	2.618	2.631	2.622 (4)
Ag3*—S3	2.653	2.655	2.707 (8)
Ag3*—S1	2.741	2.721	2.736 (5)
Ag3*—S3	2.886	2.873	2.802 (7)
Ag4—S3		2.209 (11)	2.158 (9)
Ag4—S2		2.398 (7)	2.417 (8)
Ag4—S3		2.932 (13)	3.009 (10)
Ag5*—S3			2.474 (6)
Ag5*—S1			2.543 (5)
Ag5*—S2			2.624 (6)
Ag6*—S3		2.519	2.516 (6)
Ag6*—S1		2.583	2.589 (4)
Ag6*—S2		2.716	2.735 (9)

† Ag1/Cu1—S4 distances correspond to the most probable distances given by the four S4 split positions (120 and 15 K).

Mode	*T*	*x*	*y*	*z*
Ag2*	RT	0.3786	0.1893	0.1243
	120 K	0.3616	0.1808	0.1240
Ag3*	RT	0.3303	0.3745	0.1136
	120 K	0.3257	0.3714	0.1114
Ag6*	120 K	0.2510	0.3829	0.1229

nation having two short bond distances at 2.158 (9) and 2.417 (8) Å with S3 and S2, respectively. A long contact with S3 at 3.01 (1) Å is also noticeable (Fig. 4*c*). It should be noted, however, that the short Ag4—S3 distance [2.158 (9) Å] is out of the range of Ag—S distances recalculated by Frueh (1969) on the basis of the crystal structure determinations of *ca* ten compounds with individual Ag—S bonds from 2.24 to 3.13 Å. This structural feature can be understood if one takes into account the very low occupancy factor for the Ag4 position and the large atomic displacement parameters for S3, which imply that the calculated distance does not correspond to the real distance. Ag5 (Fig. 4*d*) and Ag6 (Fig. 4*e*) are triangularly coordinated by S atoms (one S1, one S2 and one S3), having two shorter bond distances with atoms S1 and S3 [2.474 (6) and 2.543 (5) Å, and 2.516 (6) and 2.589 (4) Å, for Ag5 and Ag6, respectively] and one longer distance with atom S2 [2.624 (6) and 2.735 (9) Å, for Ag5 and Ag6, respectively]. The Ag5 and Ag6 refined positions show a more distorted crystal chemical environment than that observed for the Ag1/Cu1 position of the *A* layer. The average Ag5—S and Ag6—S distances (2.547 and 2.613 Å, respectively) are in excellent agreement with both that found for the Ag1 position in the crystal structure of stephanite, $Ag_5[S|SbS_3]$ (2.54 Å; Ribár & Nowacki, 1970), and that found for the Ag position in the crystal structure of pyrargyrite, $Ag_3[SbS_3]$ (2.573 Å; Engel & Nowacki, 1966). In addition, these distances compare reasonably well with the value of 2.66 Å extrapolated from Shannon's (1981) tables.

Finally, the Cu2 position shows a linear coordination with two distances at 2.161 (3) Å. Although these values are shorter than the sum of the ionic radii (*i.e.* 2.30 Å; Shannon, 1981), they are in excellent agreement with those found in KCuS (2.129 and 2.162 Å; Savelsberg & Schäfer, 1978), where the Cu2 atom shows a similar linear sulfur coordination that was explained through band-structure calculations by Gaudin *et al.* (2001).

6. Conclusions

The crystal structure of the mineral pearceite has been solved from X-ray single-crystal diffraction data. We showed that, as observed for the argyrodite compounds (Evain *et al.*, 1998; Gaudin *et al.*, 2000), the d^{10} cations are highly disordered, distributed along well defined diffusion-like paths joining preferred, low-coordination sites. The diffusion-like paths for silver d^{10} ions have been determined by means of a combination of a Gram–Charlier description of the atomic displacement factors and a split-atom model. As the temperature decreases the Ag cation densities condense into better defined modes but, contrary to what is commonly observed for classical ionic conductors such as argyrodite compounds, the joint probability density function still exhibits a strong overlapping of neighbouring sites and the disorder is not resolved. Ionic and electronic conductivity studies should therefore be carried out as a function of composition and temperature in order to obtain information about the transport properties of this mineral and to reach conclusions about the true nature of the disorder.

Moreover, because of the probable chemical control of the 'unit-cell type' stabilization in the minerals belonging to the pearceite–polybasite series, the effect of the isomorphic substitutions in the structure of natural samples could play a crucial role. Indeed, a different distribution of the Ag/Cu ratio in natural samples could indicate the existence of phases with strongly different structural cation disorder stabilized by diverse conditions of formation in nature.

The authors are grateful to Professor Paul G. Spry (Iowa State University, USA) for his help in electron microprobe analyses. This work was funded by MIUR, PRIN 2005 project 'Complexity in minerals: modulation, modularity, structural disorder'.

References

Becker, P. J. & Coppens, P. (1974). *Acta Cryst.* A**30**, 129–147.

Boucher, F., Evain, M. & Brec, R. (1992). *J. Solid State Chem.* **100**, 341–355.

Boucher, F., Evain, M. & Brec, R. (1993). *J. Solid State Chem.* **107**, 332–346.

Brandenburg, K. (2001). *DIAMOND*. Version 3. Crystal Impact GbR, Bonn, Germany.

Duisenberg, A. J. M., Kroon-Batenburg, L. M. J. & Schreurs, A. M. M. (2003). *J. Appl. Cryst.* **36**, 220–229.

Edenharter, A., Koto, K. & Nowacki, W. (1971). *Neues Jahrb. Mineral. Monatsh.* pp. 337–341.

Engel, P. & Nowacki, W. (1966). *Neues Jahrb. Mineral. Monatsh.* pp. 181–195.

Evain, M., Gaudin, E., Boucher, F., Petrícek, V. & Taulelle, F. (1998). *Acta Cryst.* B**54**, 376–383.

Frondel, C. (1963). *Am. Mineral.* **48**, 565–572.

Frueh, A. J. (1969). *Handbook of Geochemistry*, edited by K.-H. Wedepohl, Vol. II/4. Berlin/Heidelberg: Springer-Verlag.

Gaudin, E., Boucher, F. & Evain, M. (2001). *J. Solid State Chem.* **160**, 212–221.

Gaudin, E., Petrícek, V., Boucher, F., Taulelle, F. & Evain, M. (2000). *Acta Cryst.* B**56**, 972–979.

Hall, H. T. (1967). *Am. Mineral.* **52**, 1311–1321.

Harris, D. C., Nuffield, E. W. & Frohberg, M. H. (1965). *Can. Mineral.* **8**, 172–184.

Herrendorf, W. (1993). PhD dissertation, University of Karlsruhe, Germany.

Johnson, C. K. & Levy, H. A. (1974). *International Tables for X-ray Crystallography*, edited by J. A. Ibers & W. C. Hamilton, Vol. IV, pp. 311–336. Birmingham: Kynoch Press.

Kuhs, W. F. (1984). *Acta Cryst.* A**40**, 133–137.

Kuhs, W. F. & Heger, G. (1979). *Fast Ion Transport in Solids*, edited by P. Vashishta, J. N. Mundy & G. K. Shenoy, pp. 233–236. Amsterdam: Elsevier.

Oxford Diffraction (2002). *CrysAlis CCD* and *CrysAlis RED*, Version 1.70. Oxford Diffraction Ltd, Oxford, UK.

Peacock, M. A. & Berry, L. G. (1947). *Mineral. Mag.* **28**, 2–13.

Pertlik, F. (1994). *J. Solid State Chem.* **112**, 170–175.

Petrícek, V. & Dusek, M. (2000). *JANA2000*. Institute of Physics, Academy of Sciences of the Czech Republic, Prague, Czech Republic.

Pfitzner, A., Evain, M. & Petrícek, V. (1997). *Acta Cryst.* B**53**, 337–345.

Ribár, B. & Nowacki, W. (1970). *Acta Cryst.* B**26**, 201–207.

Savelsberg, G. & Schäfer H. (1978). *Z. Naturforsch. Teil B*, **33**, 711–713.

Shannon, R. D. (1981). *Structure and Bonding in Crystals*, edited by M. O'Keeffe & A. Navrotsky, Vol. II, pp. 53–70. New York: Academic Press.

Sheldrick, G. M. (1997). *SHELXS97*. University of Göttingen, Germany.

Stoe & Cie (1996). *X-SHAPE*. Version 1.02. Stoe & Cie, Darmstadt, Germany.